BARS DO DRIVE SPIRAL DENSITY WAVES

H. Salo[1], E. Laurikainen[1,2], R. Buta[3], and J. H. Knapen[4,5]
[1] Department of Physics/Astronomy Division, University of Oulu, FI-90014, Finland
[2] Finnish Centre for Astronomy with ESO (FINCA), University of Turku, Väisäläntie 20, FI-21500 Piikkiö, Finland
[3] Department of Physics and Astronomy, University of Alabama, Box 870324, Tuscaloosa, AL 35487, USA
[4] Instituto de Astrofísica de Canarias, E-38200 La Laguna, Tenerife, Spain
[5] Departamento de Astrofísica, Universidad de La Laguna, E-38205 La Laguna, Tenerife, Spain

ABSTRACT

Recently, Buta et al. examined the question "Do Bars Drive Spiral Density Waves?", an idea supported by theoretical studies and also from a preliminary observational analysis. They estimated maximum bar strengths Q_b, maximum spiral strengths Q_s, and maximum $m = 2$ arm contrasts A_{2s} for 23 galaxies with deep Anglo-Australian Telescope (AAT) K_s-band images. These were combined with previously published Q_b and Q_s values for 147 galaxies from the Ohio State University Bright Spiral Galaxy Survey (OSUBSGS) sample and with the 12 galaxies from Block et al. Weak correlation between Q_b and Q_s was confirmed for the combined sample, whereas the AAT subset alone showed no significant correlations between Q_b and Q_s, nor between Q_b and A_{2s}. A similar negative result was obtained in Durbala et al. for 46 galaxies. Based on these studies, the answer to the above question remains uncertain. Here we use a novel approach, and show that although the correlation between the *maximum* bar and spiral parameters is weak, these parameters do correlate when compared *locally*. For the OSUBSGS sample, a statistically significant correlation is found between the local spiral amplitude, and the forcing due to the bar's potential at the same distance, out to ≈ 1.6 bar radii (the typical bar perturbation is then of the order of a few percent). Also for the sample of 23 AAT galaxies of Buta et al., we find a significant correlation between local parameters out to ≈ 1.4 bar radii. Our new results confirm that, at least in a statistical sense, bars do indeed drive spiral density waves.

Key words: galaxies: kinematics and dynamics – galaxies: spiral – galaxies: structure

1. INTRODUCTION

The response of an outer disk to a rotating bar is intimately related to the maintenance of long-lasting spiral arms in galaxies. Optical photometry (Schweizer 1976) established that besides the gas and young stars, the spirals are also present in the old population. This was confirmed by near-infrared surveys (Eskridge et al. 2002), and is particularly true for grand-design spirals (Knapen & Beckman 1996). Short-lived stellar density waves can be induced via disk instabilities (Bertin et al. 1977; Goldreich & Tremaine 1978), or by galaxy interactions (Toomre & Toomre 1972), but such transient patterns fade after ∼10 galaxy rotations (Sellwood & Carlberg 1984), unless they are maintained by some feedback cycle, e.g., due to the swing amplification (Toomre 1981). On the other hand, spiral arms are excited by a growing bar, as demonstrated by the very first *N*-body simulations (Hohl 1971) and by analytical calculations (Athanassoula 1980).

Support for the bar/spiral connection is provided by the examples where prominent spirals extend from the ends of the bar (see, e.g., NGC 1300, p. 525 in Binney & Tremaine 2008, or NGC 986 in Buta et al. 2010). Also, grand-design spirals are more frequent in barred than in non-barred galaxies (Elmegreen & Elmegreen 1982). Nevertheless, a direct connection between bars and spirals has been difficult to prove observationally.

The possible driving of spirals by bars was addressed by Block et al. (2004), who compared the maximum of bar-related torque strength Q_b (the maximum of tangential force amplitude normalized by mean radial force) with the maximum associated with the spirals, Q_s, after separating the bar and spiral components based on their Fourier density amplitude profiles. Near-IR observations were used to show the effect of the bar

on the surrounding mass rather than on the gas or the formation of young stars. Based on 12 galaxies observed in the K_s band, Block et al. (2004) found a strikingly clear correlation between Q_b and Q_s. However, the correlation is less clear in later studies using larger samples and deeper images. In Buta et al. (2005), we analyzed the *H*-band images from the Ohio State University Bright Spiral Galaxy Survey (OSUBSGS; Eskridge et al. 2002) for 147 galaxies, and were able to "weakly verify a possible correlation between Q_s and Q_b." More recently, in Buta et al. (2009), we analyzed deep K_s Anglo-Australian Telescope (AAT) observations for 23 galaxies, with no statistically significant correlation between Q_b and Q_s, nor between Q_b and A_{2s} (the maximum of $m = 2$ Fourier density amplitude of spirals). Similarly, Durbala et al. (2009) found no correlations when analyzing Sloan *i*-band data for 46 isolated barred galaxies; a lack of correlation between bar and spiral arm strengths was also seen by Seiger et al. (2003) who analyzed 41 galaxies. Nevertheless, Buta et al. (2009) showed that the correlation is present when combining the AAT data with the previous data sets of Block et al. (2004) and Buta et al. (2005).

In this paper, the bar/spiral connection is re-investigated using the same samples which were used by Buta et al. (2005, 2009): the OSUBSGS sample containing ∼100 barred galaxies, and our AAT sample of 23 barred galaxies. A novel approach is used: instead of comparing the *maximum* bar strength with the *maximum* spiral density amplitude, we compare the locally measured bar forcing and spiral amplitude as a function of distance. The locally felt forcing due to the bar is a more important parameter than the maximum forcing, since Q_b is typically attained well inside the spiral structure. Also, we examine the spiral density rather than force amplitude, since the former more directly measures the possible *response* to

bar forcing. Using our approach, a statistically significant correlation is demonstrated to exist between the bar forcing and the spiral amplitude, up to a considerable distance beyond the end of the bar.

2. CALCULATION OF BAR FORCING AND SPIRAL AMPLITUDES

We calculate the amplitude of the bar tangential forcing as a function of distance from the galaxy center, $Q_{bar}(r)$, and compare it to the $m = 2$ surface brightness amplitude of the spirals, $A_2(r)$, at the same radial distances, normalized to bar radius, r/R_{bar}. The Spearman rank correlation coefficient r_s between Q_{bar} and A_2 and its significance level are then measured as a function of r/R_{bar}. A non-parametric test is used in order to avoid making assumptions about the distributions of the compared quantities. The distance up to which a significant correlation is found is regarded as a statistical estimate of the region inside which bars are able to drive spiral structure.

We use near-IR images to evaluate the galaxy potential, and derive the tangential force amplitude at each distance, normalized to the azimuthally averaged radial force

$$Q_{bar}(r) = \frac{\max(|F_T(r, \varphi)|)}{\langle|F_R(r, \varphi)|\rangle}.$$

Several assumptions are made: (1) the mass-to-luminosity ratio (M/L) is constant; (2) the vertical profile of the disk and the bar is approximated with an exponential function; and (3) the vertical scale height, h_z, scales with the galaxy size as $h_z = 0.1 R_{K20}$ (Speltincx et al. 2008), where R_{K20} is the $m_K = 20$ isophotal radius from Two Micron All Sky Survey (Skrutskie et al. 2006). The calculations are made with polar integration (Salo et al. 1999; Laurikainen & Salo 2002), based on azimuthal Fourier decomposition of the deprojected image

$$I(r, \varphi) = A_0(r)\left[1 + \sum_{m=1}^{\infty} A_m(r)\cos\left(m\left[\varphi - \varphi_m(r)\right]\right)\right],$$

which also provides the $m = 2$ Fourier density profile used to characterize the spiral amplitudes (note the normalization). The gravity is separately calculated for each m component (using $m = 0, 2, 4, 6, 8, 10$) and added together. Compared to direct Cartesian integration, the polar method effectively suppresses the spurious force maxima which otherwise could arise in the noisy outer disks (Salo et al. 2004). To account for the different three-dimensional distribution of the bulge light, multi-component decompositions are used (Laurikainen et al. 2005), reducing the artificial tangential force amplitudes arising from the bulge deprojection stretch. The polar method also makes it easy to exclude the contribution of spirals on the calculation of Q_{bar}, by setting the $m > 0$ Fourier density amplitudes to zero beyond a certain cutting distance, R_{cut}, representing the end of the bar.

Our method is illustrated in Figure 1, where the radial profiles of the $m = 2$ and $m = 4$ Fourier density amplitudes, and the Q_{bar} ratio are shown for NGC 1566. In this particular example, the A_2 and the A_4 have two well-separated local maxima associated with the bar and the spiral, but the distinction is not always clear. The Q_{bar} profile is constructed both for the total (bar+spiral) force field, and without the contribution of the spiral arms. The bar-only profile is obtained using a cutting distance $R_{cut} = R_{bar}$ in the force calculation. Our method of isolating the bar forcing is different from that of Buta et al. (2003, 2005, 2009), who
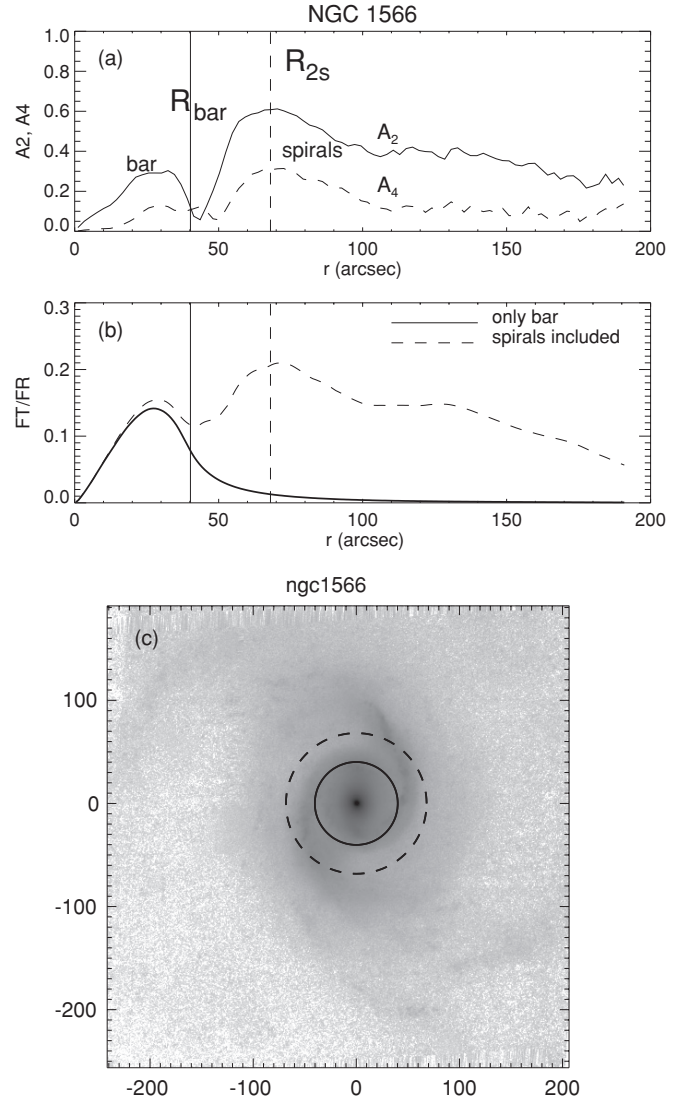

Figure 1. Barred galaxy NGC 1566, with strong outer spirals. In (a), the normalized A_2 and A_4 Fourier amplitudes are shown as a function of radius. The two local maxima are associated with the bar and the spiral: the vertical lines indicate the bar length R_{bar}, and the distance of maximum A_2 of the spirals (R_{2s}). (b) The calculated tangential forcing $Q_{bar} = F_T/F_R$, with and without the contribution from spiral arms: in the latter case, the $m > 0$ Fourier components have been set to zero for $r > R_{cut}$, here using $R_{cut} = R_{bar}$. (c) The deprojected K_s-band image (Buta et al. 2009), together with circles of radii R_{bar} and R_{2s}.

extrapolated the bar density into the spiral region based on Gaussian fits to Fourier density profiles. Here, we assume that the bar and the spiral dominate their radial domains with no significant overlap.

3. BAR-DRIVEN SPIRAL STRUCTURE IN THE OSUBSGS AND AAT SAMPLES

The OSUBSGS is a magnitude-limited sample ($m_B < 12.0$ mag) of galaxies with Hubble types $0 \leqslant T \leqslant 9$. The H-band images typically reach 20 mag arcsec^{-2} in depth. Our bar identifications and lengths are from Table 3 in Laurikainen et al. (2004), and are based on the Fourier amplitude and phase profiles ("Fourier bars"; NGC 2207 was omitted, leaving 103 galaxies for analysis).

A statistically significant correlation is found between the amplitude A_2, and the bar forcing, Q_{bar}, when these parameters are compared at the same radial distances. See Figure 2 where
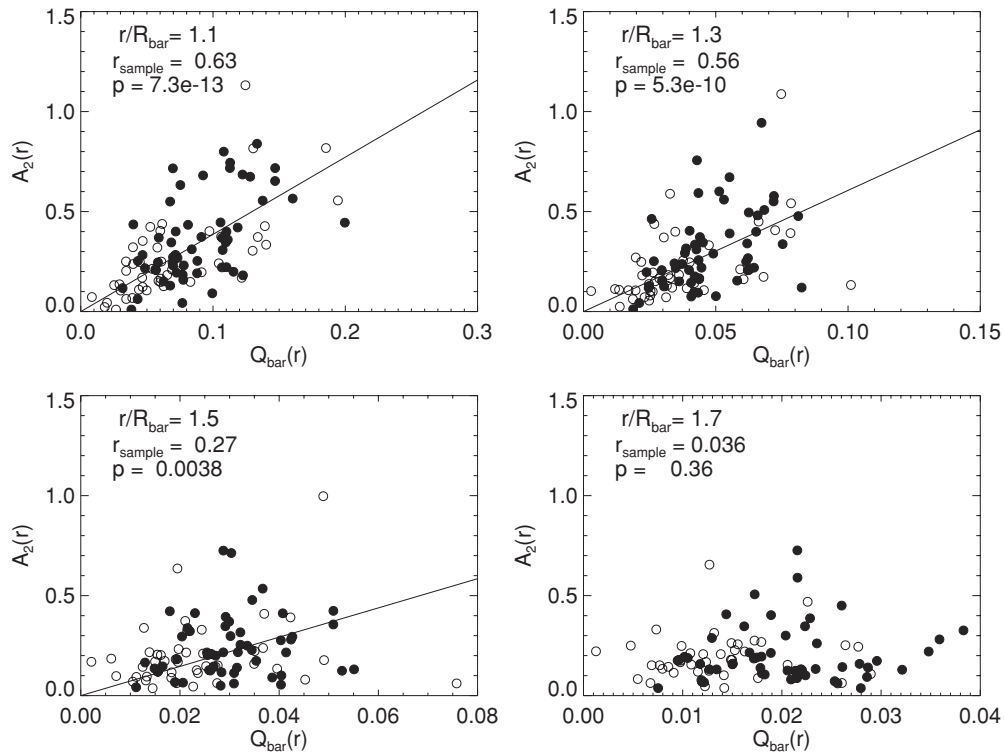
Figure 2. Relation between local bar forcing and local spiral amplitude. Four distances, normalized to the bar length ($r/R_{bar} = 1.1$–1.7) are compared, for the 103 barred OSUBSGS galaxies. In the calculation of bar forcing, the $m > 0$ density Fourier amplitudes are set to zero beyond $R_{cut} = R_{bar}$. The p values indicate the significance of the Spearman rank correlation coefficient r_{sample} (the probability of having $r_s > r_{sample}$ is p, under the hypothesis that the variables are independent). In the case where $p < 0.01$, the best-fit linear relation is also indicated. Open and filled circles denote short ($R_{bar}/h_R < 1$) and long bars ($R_{bar}/h_R > 1$), showing no difference.

the different panels represent examples of measurements at successively larger radial distances with respect to the bar. The bar force is cut using $R_{cut} = R_{bar}$, which means that we are conservative in eliminating any contamination by the spiral arms themselves in the forcing. The correlation is very strong just beyond the bar, and stays statistically significant until $\sim 1.6\,R_{bar}$ (rank correlation coefficient $r_s = 0.25$, significance $p = 0.008$). The correlation is similar for long ($R_{bar}/h_R > 1$) and short ($R_{bar}/h_R < 1$) bars, when normalized to the disk scale length. The range of the significant correlation is also similar for early- ($T \leqslant 3$) and late-type ($T \geqslant 4$) spirals (not shown in the plots).

Figure 3 collects the correlation coefficients between A_2 and Q_{bar} at different distances r/R_{bar}. Note that in the bar region, where A_2 represents the bar itself, the correlation is strong as expected. Outside the bar, A_2 arises from spiral structures (the forcing is still dominated by the bar). The radial trend depends only slightly on the adopted cutting distance for the bar (using reasonable values $R_{cut}/R_{bar} = 1.0$–1.2). The correlation is also insensitive to the exact assumptions made about vertical structure: an uncertainty by a factor of 2 in h_z corresponds to $\sim 20\%$ uncertainty in bar strength. Monte Carlo trials show that even 20% random errors in Q_{bar} (and A_2) affect only marginally the significance of the correlation (for 10,000 trials, the median $p = 0.023$ for $r = 1.6\,R_{bar}$).

We made a similar analysis for the AAT sample of 23 barred galaxies, using the data and bar lengths from Buta et al. (2009). The K_s-band images typically reach a surface brightness level of 22–24 mag arcsec^{-2}. The sample covers a wide range of bar strengths, extending to strongly barred galaxies, for which case a strongest correlation between Q_{bar} and A_2 is expected. However, as discussed in Buta et al. (2009), no statistically
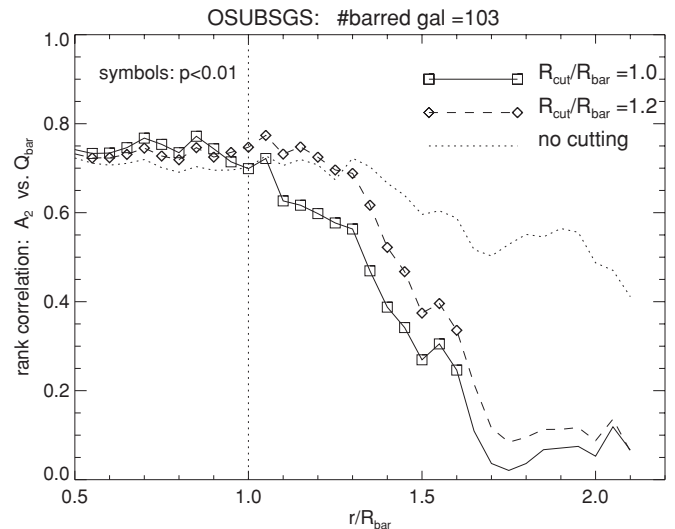

Figure 3. Rank correlation coefficient between the local bar forcing $Q_{bar}(r)$ and the local amplitude $A_2(r)$, as a function of distance r/R_{bar}. Note that at $r/R_{bar} < 1$ the parameter A_2 describes the bar density contrast, whereas outside the bar it describes the spiral arms. Symbols indicate statistically significant correlation, obtained for $r \leqslant 1.6\,R_{bar}$. Note that the result is independent of the exact manner in which the spiral contribution has been eliminated from the bar forcing: compare the solid ($R_{cut} = R_{bar}$) and dashed ($R_{cut} = 1.2\,R_{bar}$) curves. Also shown is the case with no cutting (dotted line): this is just for comparison, since the calculated forcing is then strongly affected by the spirals themselves.

significant correlation is obtained between the maximum of Q_{bar} and the maximum of A_2 (Figure 4(a)). The result is similar for galaxies having the maximum spiral amplitude nearer
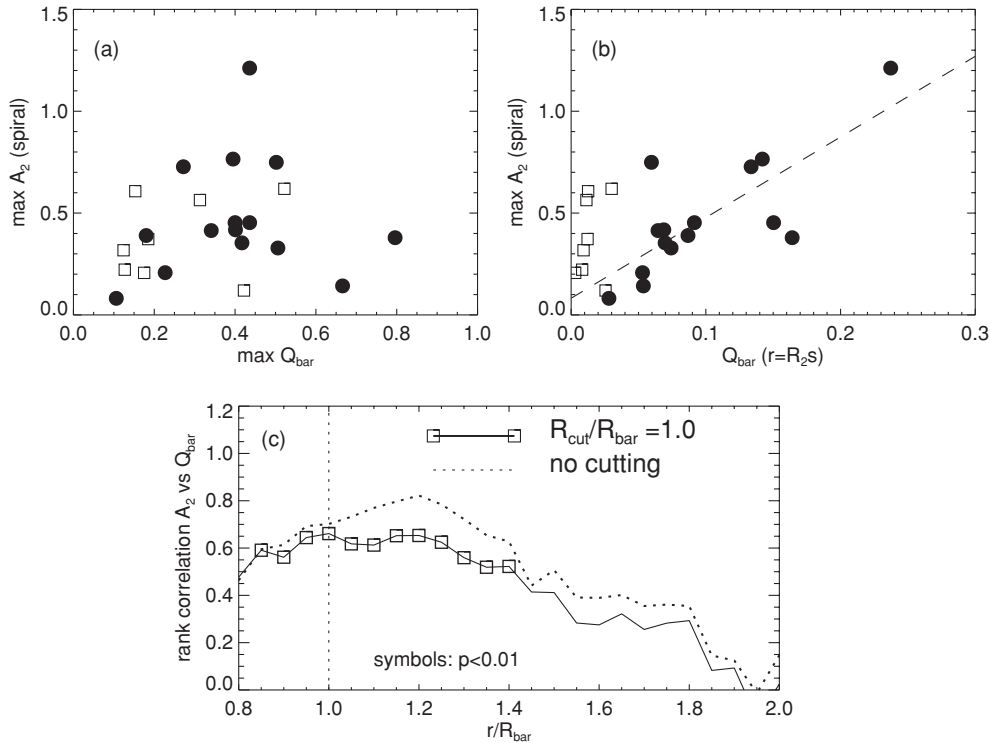
Figure 4. Re-analysis of the AAT sample of 23 barred galaxies. The separation of bar and spiral components in Buta et al. (2009) yielded the maximum of bar forcing Q_{bar} and the maximum of spiral amplitude A_2, the latter attained at distance R_{2s}. Frame (a) indicates no correlation between these quantities (same data as in Figure 26(a) in Buta et al.). The filled and open symbols distinguish the galaxies with $R_{2s}/R_{bar} < 1.5$ and $R_{2s}/R_{bar} > 1.5$, respectively. (b) However, a correlation is present (with a significance $p = 0.007$) if we compare the bar forcing at the location of the maximum spiral amplitude; this is particularly clear for galaxies with $R_{2s}/R_{bar} < 1.5$ (filled symbols). (c) The connection of bars and spirals is even clearer if the local bar forcing and local spiral amplitude are compared as a function of distance: the figure shows the rank correlation coefficient vs. distance, constructed in the same manner as in Figures 2 and 3.

($R_{2s} < 1.5 R_{bar}$) or further ($R_{2s} > 1.5 R_{bar}$) outside the bar. However, a statistically significant correlation is found if the *local* bar forcing at the location of the maximum spiral amplitude is examined (Figure 4(b)). The correlation is particularly clear if we limit to cases where $R_{2s} < 1.5 R_{bar}$. This is in accordance with our result for the OSUBSGS where a statistical dependence is present but discernible only up to certain distance beyond the bar end. Indeed, if we repeat the analysis we made for the OSUBSGS sample (Figure 4(c)), a statistically significant correlation is found between $Q_{bar}(r)$ and $A_2(r)$ up to 1.4 R_{bar}. The somewhat smaller range in the AAT analysis is probably due to the smaller sample size in comparison to the OSUBSGS sample.

4. DISCUSSION

4.1. Comparison to Previous Studies of Bar/Spiral Correlation

Our analysis for OSUBSGS has indicated a significant correlation between the *local* tangential bar force $Q_{bar}(r)$ and the *local* surface brightness Fourier amplitude $A_2(r)$, up to 1.6 R_{bar}. How does this compare to the previous analyses of Q_b versus Q_s, some of which indicated a correlation, while others did not? In Buta et al. (2005), we did not explicitly state the correlation coefficient, but using the data tabulated in the paper one finds a Pearson linear correlation coefficient $r = 0.35$. For a sample of $N = 146$ galaxies, this implies a very significant correlation ($p = 0.8 \times 10^{-5}$). Though different quantities are compared, this statistically significant correlation between maximum values agrees with our present analysis of the correlation between local quantities.

Likewise, the negative results in Buta et al. (2009) for the AAT sample alone ($N = 23$), and in Durbala et al. (2009) for the Sloan sample ($N = 46$), are accounted for by the smaller number of galaxies. The standard procedure for testing the significance of a positive linear correlation (see, e.g., Wall & Jenkins 2003, Section 4.2.2) implies that in order to accept the correlation (at a significance level $p < 0.01$), the sample correlation coefficients must be $r > 0.48$ and $r > 0.34$, for $N = 23$ and $N = 46$, respectively. Assume for a while that a linear correlation between Q_b and Q_s exists, and that these quantities are drawn from a bivariate-Gaussian distribution with an actual correlation coefficient $\rho = 0.35$ (equal to the sample correlation coefficient in Buta et al. 2005). We may then ask what the odds are of detecting this correlation, i.e., of observing a sufficiently high sample correlation when drawing a random sample with different N's. Applying the Fisher probability distribution for the sample r with a known ρ (Wall & Jenkins 2003) implies that for $N = 23$ there is only a 25% chance of detecting the correlation, even for $N = 46$ the change is only about 50%. If we use the rank correlation coefficient instead of the linear correlation coefficient, the chances are reduced to 15%–38%, respectively (obtained by Monte Carlo trial estimates). Thus, the negative results for these small samples do not rule out true correlations.

The current method seems to be capable of exposing the correlation even for fairly small samples, indicating the advantage of comparing the local quantities. In particular, close to the bar the spiral amplitudes are strongly correlated with the bar forcing. This radial dependence of the correlation probably explains the very strong correlation found in Block et al. (2004). The fact

that their small sample ($N = 12$) showed the strongest correlation ($r = 0.86$) is likely to result from the way the galaxies were selected, containing many examples where the spirals are strong right at the ends of the bar. Indeed, according to the tabulated values in their paper, the mean ratio between the radial locations of the spiral and bar maximum forces was $\langle R_s/R_b \rangle = 2.5$, compared to $\langle R_s/R_b \rangle = 4.6$ in Buta et al. (2005), which was based on a magnitude-limited sample of spirals, with many different types of bar/spirals.

4.2. Physical Mechanisms

Our observational analysis indicates a clear statistical relation between bars and spirals. At least the following mechanisms might account for this.

1. Spiral structure is a direct response to bar forcing and/or the spirals represent a continuation of the density wave associated with the bar (Lindblad 1960; Toomre 1969; Bertin & Lin 1996). Recently, spiral arms have also been interpreted as manifold orbits emanating from unstable Lagrangian points near the bar ends (Romero-Gómez et al. 2006; Athanassoula et al. 2009).
2. Spirals are coupled to the bar via non-linear resonance coupling (Tagger et al. 1987; Masset & Tagger 1997). Such couplings are seen in N-body simulations (Rautiainen & Salo 1999), but it is uncertain how frequent such cases really are.

The first explanation is likely to apply to the strong correlation just outside the bar. In this case, the spirals are expected to share the constant (or slowly evolving) pattern speed of the bar. Similarly, in the case of non-linear coupling, though the spiral pattern speed is slower than that of the bar, it still represents a steady long-lived pattern. On the other hand, in the region where no correlation is present, the spirals are independent structures, representing either a long-lasting mode with a slower pattern speed than the bar (Sellwood & Sparke 1988), or are just short-lived transient wave packets with a range of propagation speeds (Sellwood & Kahn 1991; Salo & Laurikainen 2000).

Note that some correlation may be present even if bars and spirals are independent, since both types of structures are favored by gravitationally more reactive disks. Nevertheless, in this case, a correlation between maximum values would also be expected.

Sellwood (2008) discusses the importance of distinguishing between long-lived spiral modes and transient waves. This stems from the fact that the latter are much more efficient in driving angular momentum transport in the disk. In case of steady patterns, the angular momentum exchange with stars is limited to resonances, whereas in the case of transient patterns this may occur over a large range of radii. Multiple transient patterns also lead to radial mixing of stars, as well as secular heating of the disk.

In the current samples, no significant correlation is seen beyond $\sim$1.6 R_{bar}, at which distance the typical force amplitudes associated with the bar fall below a few percent level. This provides an observational lower estimate for the extent of bar-driving. Namely, in the outer disk, the determination of the spiral amplitude is more prone to uncertainties due to image noise and background subtraction, diluting any correlation that may be present. Also, we are fairly conservative in cutting the bar contribution close to R_{bar}, since in the case where the spiral arms are a part of the mode associated with the bar, the local spiral forcing would also contribute to maintaining the pattern.

Although the correlation we find is strictly statistical, it is interesting to consider how it applies to the individual example of NGC 1566, shown in Figure 1. For this galaxy $R_{\mathrm{bar}} = 40''$, and the A_2 maximum related to the strong spirals is at $R_{2s} = 68''$ (Buta et al. 2009), though there are additional spiral arms even beyond $100''$. The strong spirals, with a maximum at 1.7 bar lengths, fall marginally in the region where bar-driving is expected. Continuing the same interpretation, the spiral beyond $\sim$100$''$ would be an independent pattern. Indeed, NGC 1566 has been quoted as an example of a galaxy with at least two separate spiral structures (Bosma 1992).

5. CONCLUSIONS

A connection between bar forcing and spiral density amplitudes was investigated for two near-infrared galaxy samples: 103 barred galaxies from the magnitude-limited OSUBSGS survey, and 23 barred galaxies in our AAT Survey. The main results are as follows.

1. For both samples, a statistically significant correlation is found between the local tangential bar forcing, $Q_{\mathrm{bar}}(r)$, and the local spiral amplitude, $A_2(r)$, up to a radial distance of $r \sim 1.5 R_{\mathrm{bar}}$.
   The correlation suggests that, at least in a statistical sense, the stellar spirals of the disk are not transient features but rather represent a continuation of the bar mode itself, or are driven by the bar through some mechanism. Further out, the spirals may be either independent modes or transient wave packets.
2. The obtained range of the correlation is similar for early- and late-type spirals ($0 \leqslant T \leqslant 3$ and $4 \leqslant T \leqslant 9$), and also for small and large bars (R_{bar}/h_r smaller/larger than unity).

This does not favor the idea that only certain types of bars could drive spiral structure, or that the forcing on the stellar component requires the presence of significant gas component. Nevertheless, the current samples are small, and a larger number of galaxies is needed to draw reliable conclusions about morphological-type dependencies, or to probe whether the statistical correlation extends to even larger distances beyond the bar. In this respect, the forthcoming S^{4}G survey (The Spitzer Survey of Stellar Structure in Galaxies; Sheth 2009, Sheth et al. 2010) will be extremely useful, providing unprecedentedly deep 3.6 and 4.5 μm observations for nearly 2300 nearby galaxies.

REFERENCES

Athanassoula, E. 1980, A&A, 88, 184
Athanassoula, E., Romero-Gómez, M., Bosma, A., & Masdemont, J. J. 2009, MNRAS, 400, 1706
Bertin, G., Lau, Y. Y., Lin, C. C., Mark, J. W.-K., & Sugiyama, L. 1977, Proc. Natl. Acad. Sci., 74, 4726
Bertin, G., & Lin, C. C. 1996, Spiral Structure in Galaxies: A Density Wave Theory (Cambridge, MA: MIT Press)
Binney, J., & Tremaine, S. 2008, Galactic Dynamics (2nd ed.; Princeton, NJ: Princeton Univ. Press)
Block, D. L., Buta, R., Knapen, J. H., Elmegreen, D. M., Elmegreen, B. G., & Puerari, I. 2004, AJ, 128, 183
Bosma, A. 1992, in Morphological and Physical Classification of Galaxies, ed. G. Longo, M. Capaccioli, & G. Busarello (Dordrecht: Kluwer), 207
Buta, R., Block, D. L., & Knapen, J. H. 2003, AJ, 126, 1148
Buta, R., Knapen, J. H., Elmegreen, B. G., Salo, H., Laurikainen, E., Elmegreen, D. M., Puerari, I., & Block, D. L. 2009, AJ, 137, 4487
Buta, R., Vasylyev, S., Salo, H., & Laurikainen, E. 2005, AJ, 130, 506
Buta, R., et al. 2010, ApJS, submitted
Durbala, A., Buta, R., Sulentic, J. W., & Verdes-Montenegro, L. 2009, MNRAS, 397, 1756

Elmegreen, D. M., & Elmegreen, B. G. 1982, MNRAS, 201, 1035
Eskridge, P. B., et al. 2002, ApJS, 143, 73
Goldreich, P., & Tremaine, S. 1978, ApJ, 222, 850
Hohl, F. 1971, ApJ, 168, 343
Knapen, J., & Beckman, J. E. 1996, MNRAS, 283, 251
Laurikainen, E., & Salo, H. 2002, MNRAS, 337, 1118
Laurikainen, E., Salo, H., & Buta, R. 2005, MNRAS, 362, 1319
Laurikainen, E., Salo, H., Buta, R., & Vasylyev, S. 2004, MNRAS, 355, 1251
Lindblad, P. O. 1960, Stockholm Obs. Ann., 21, 4
Masset, F., & Tagger, M. 1997, A&A, 322, 442
Rautiainen, P., & Salo, H. 1999, A&A, 348, 737
Romero-Gómez, M., Masdemont, J. J., Athanassoula, E., & García-Gómez, C. 2006, A&A, 453, 39
Salo, H., & Laurikainen, E. 2000, MNRAS, 319, 393
Salo, H., Laurikainen, E., & Buta, R. 2004, in ASSL 319, Penetrating Bars Through Masks of Cosmic Dust., ed. L. Block et al. (Dordrecht: Kluwer), 673
Salo, H., Rautiainen, P., Buta, R., Purcell, G. B., Cobb, M. L., Crocker, D. A., & Laurikainen, E. 1999, AJ, 117, 792

Schweizer, F. 1976, ApJS, 31, 313
Seiger, M. S., Chorney, N. E., & James, P. A. 2003, MNRAS, 342, 1
Sellwood, J. A. 2008, in ASP Conf. Ser. 396, Dynamical Evolution of Disk Galaxies, ed. G. Funes & E. M. Corsini (San Francisco, CA: ASP)
Sellwood, J. A., & Carlberg, R. G. 1984, ApJ, 282, 61
Sellwood, J. A, & Kahn, L. S. 1991, MNRAS, 250, 278
Sellwood, J. A., & Sparke, L. S. 1988, MNRAS, 231, 25
Sheth, K. 2009, BAAS, 41, 711
Sheth, K., et al. 2010, PASP, submitted
Skrutskie, M. F., et al. 2006, AJ, 131, 1163
Speltincx, T., Laurikainen, E., & Salo, H. 2008, MNRAS, 383, 317
Tagger, M., Sygnet, J. F., Athanassoula, E., & Pellat, R. 1987, ApJ, 318, L43
Toomre, A. 1969, ApJ, 158, 899
Toomre, A. 1981, in The Structure and Evolution of Normal Galaxies, ed. S. M. Fall (Cambridge: Cambridge Univ. Press), 111
Toomre, A., & Toomre, J. 1972, ApJ, 178, 623
Wall, J. V., & Jenkins, C. R. 2003, Practical Statistics for Astronomers (Cambridge: Cambridge Univ. Press)